# Compress-and-Forward via Multilevel Coding

Heping Wan<sup>†</sup>, Anders Høst-Madsen<sup>††</sup>, and Aria Nosratinia<sup>†</sup>

†Department of Electrical Engineering, The University of Texas at Dallas, Richardson, TX, USA

Email: {Heping.Wan, aria}@utdallas.edu

††Department of Electrical Engineering, University of Hawaii, Manoa, Honolulu, HI, USA

Email: ahm@hawaii.edu

Abstract—We investigate the performance of discrete (coded) modulations in the full-duplex compress-forward relay channel using multilevel coding. We numerically analyze the rates assigned to component binary codes of all levels. LDPC codes are used as the component binary codes to provide error protection. The compression at the relay is done via a nested scalar quantizer whose output is mapped to a codeword through LDPC codes. A compound Tanner graphical model and information-exchange algorithm are described for joint decoding of both messages sent from the source and relay. Simulation results show that the performance of the proposed system based on multilevel coding is better than that based on BICM, and is separated from the SNR threshold of the known CF achievable rate by two factors consisting approximately of the sum of the shaping gain (due to scalar quantization) and the separation of the LDPC code implementation from AWGN capacity.

#### I. Introduction

After the introduction of the three-node relay channel by Van Der Meulen [1], several coding protocols [2] including the decode-and-forward (DF) and compress-and-forward (CF) have been proposed for the relay channel. DF is capacity achieving for the degraded relay channel [2]. However, DF performs worse than CF does when the source-relay link is weak, since the relay must perfectly decode the message sent from the source in DF, while in CF the relay employs the side information provided by the destination to compress received sequence.

There are some prior works on coding techniques for implementing CF. In [3] [4] and [5], a half-duplex relay uses Wyner-Ziv coding to compress the received sequence, and the destination uses successive decoding to first decode the message sent from the relay which will help to decode the message sent from the source. In [3] and [4], LDPC codes are used for channel coding at the source, and the combination of nested scalar quantization and irregular-repeat accumulation (IRA) codes is used by the relay to implement Wyner-Ziv coding and channel coding. In [5], a nested construction of polar codes is used to implement channel coding and Wyner-Ziv coding over the relay channel with orthogonal receiver components.

In [6] and [7], the half-duplex relay implements a different compression strategy by mapping quantized sequence to a codeword, and joint decoding of both messages sent from the source and relay is applied by the destination. In their work, LDPC codes are used for channel coding at the source, LDPC codes [6] or low density generator matrix (LDGM) codes [7]

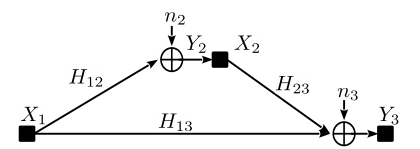


Fig. 1. Full-duplex Gaussian relay channel

are used for mapping the quantized sequence to a codeword, and a compound Tanner graph is derived to implement joint decoding at the destination. In addition, this binary framework is extended to the half-duplex relay channel with bit-interleaved coded modulation (BICM) by decomposing the original channel into parallel independent binary sub-channels.

In this paper, we aim to investigate the performance of discrete (coded) modulations in the full-duplex CF relay channel in the presence of additive white Gaussian noise (AWGN). In particular, we analyze, design, and simulate multilevel coding (MLC) [8] as a convenient and flexible method for the implementation of coded modulation in this multi-node network. We numerically analyze the proper assignment of rates to the component binary codes of all levels, while the component binary codes of the same rate are used in all subchannels in [6] and [7]. In our scheme, LDPC codes are used for error protection at the source, and mapping the output of an nested scalar quantizer to a codeword whose parity bits are tranmitted at the relay. A compound Tanner graphical model composed of two LDPC Tanner graphs and corresponding information-exchange algorithm are derived for joint decoding at the destination. The rest of the paper is organized as follows. In Section II, the relay channel model and CF relay are described. Achievable rates and the rates assigned to all levels are computed and analyzed. Section III details the implementation of the CF relay, with the emphasis on the compound Tanner graphical model and information-exchange algorithm involved in decoding. In Section IV, simulation results are presented and discussed. Section V concludes the paper.

# II. PRELIMINARIES

The three-node full-duplex relay channel with AWGN and constellation-constraint input is shown in Fig. 1. The source transmits  $X_1 \in \mathcal{A}$  satisfying power constraint  $P_s$  to the destination and relay. The relay transmits  $X_2 \in \mathcal{B}$  satisfying power constraint  $P_r$  to the destination.  $\mathcal{A}$  and  $\mathcal{B}$  denote the

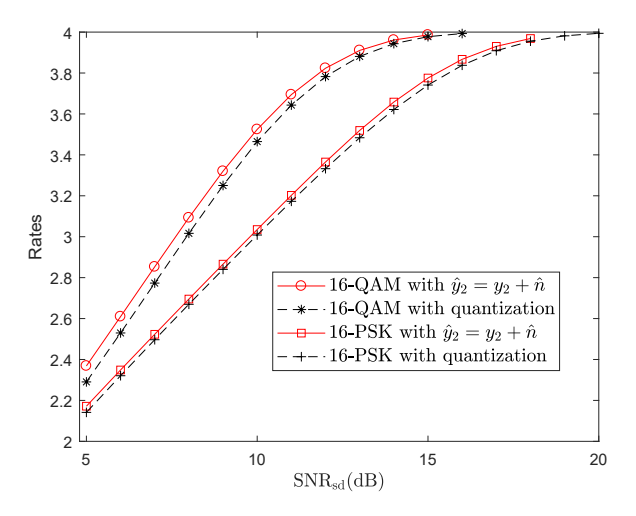


Fig. 2. CF achievable rates versus  ${\rm SNR_{sd}}$  for 16-QAM and 16-PSK with  $N_3=1,~N_2=8,~H_{13}=1,~H_{12}=2,~H_{23}=11,$  and  $P_r=P_s.$ 

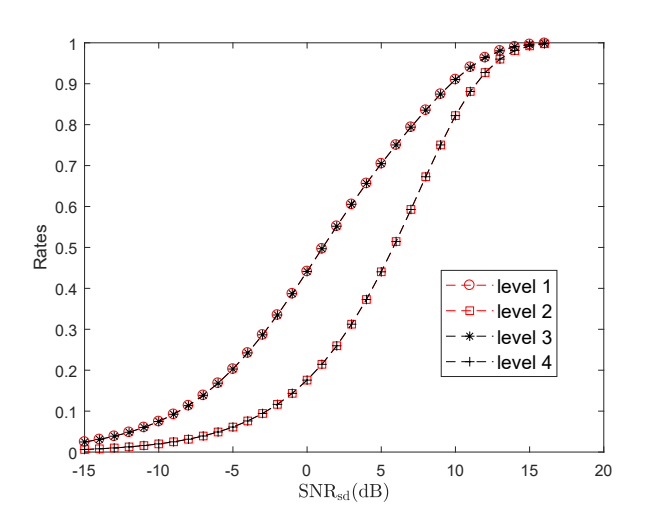


Fig. 3. Level-wise achievable rates from the most to least significant bit with 16-QAM,  $N_3=1,\ N_2=8,\ H_{13}=1,\ H_{12}=2,\ H_{23}=11,$  and  $P_r=P_s$ .

constellation alphabets of  $X_1$  and  $X_2$  respectively.  $n_2$  and  $n_3$  are AWGN with zero mean and variance  $N_2$  and  $N_3$ . The received signals of the relay and destination at block t are modeled as

$$Y_2^{(t)} = H_{12}X_1^{(t)} + n_2, (1)$$

$$Y_3^{(t)} = H_{13}X_1^{(t)} + H_{23}X_2^{(t-1)} + n_3, (2)$$

where  $H_{13}$ ,  $H_{12}$  and  $H_{23}$  are corresponding channel coefficients as illustrated in Fig. 1.

## A. CF with nested scalar quantization

The coding strategy for CF is described as follows.

At block t, the source maps one of  $2^{nR}$  messages to a length n codeword  $\mathbf{X}_1^{(t)}$ , and transmits  $\mathbf{X}_1^{(t)}$  to the destination and relay. Due to causality, the relay reconstructs the received sequence at block t-1.  $\hat{\mathbf{Y}}_2^{(t-1)}$  denotes the reconstruction

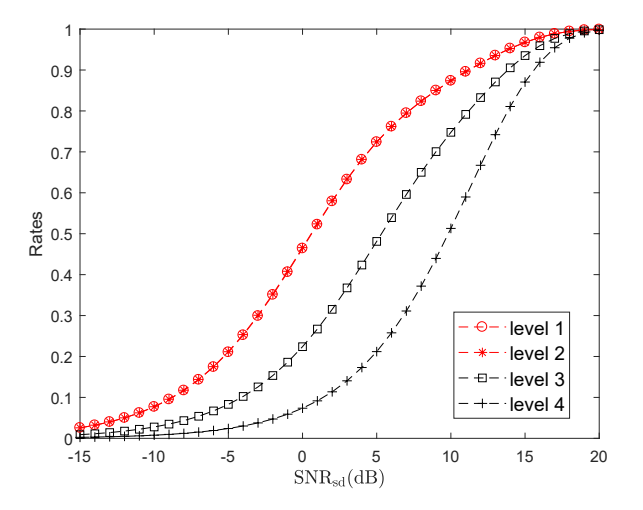


Fig. 4. Level-wise achievable rates from the most to least significant bit with 16-PSK,  $N_3=1,\ N_2=8,\ H_{13}=1,\ H_{12}=2,\ H_{23}=11,\ {\rm and}\ P_r=P_s.$ 

sequence of  $\mathbf{Y}_2^{(t-1)}$ . Then  $\hat{\mathbf{Y}}_2^{(t-1)}$  is mapped to a length n codeword  $\mathbf{X}_2^{(t-1)}$  which is transmitted to the destination. At block t, the destination uses joint decoding to recover the source message sent at block t-1. The achievable rate is [9, Section 16.7]

$$R < \max I(X_1; \hat{Y}_2, Y_3 | X_2),$$
 (3)

subject to the constraint  $I(Y_2; \hat{Y}_2 | X_2, Y_3) \leq I(X_2; Y_3)$ , where the maximum is over all conditional pmfs  $p(x_1)p(x_2)p(\hat{y}_2 | x_2, y_2)$ .

In our work, the reconstruction sequence is obtained by feeding the received sequence into an nested scalar quantizer [10] having L output indices. If the received signal  $Y_2$  is complex, we need to independently design two sub-quantizers with both having  $\sqrt{L}$  output indices for the real and imaginary parts of  $Y_2 = Y_{2,R} + i \times Y_{2,I}$ , where  $i = \sqrt{-1}$ . When

$$Y_{2,R} \in \bigcup_{k=-\infty}^{\infty} \{x : x \in \mathbb{R}, 0 \le x - (\omega + k\sqrt{L})q_1 \le q_1\},$$

where  $q_1$  is the quantization step size, the sub-quantizer for the real part outputs  $\omega \in \{0, 1, ..., \sqrt{L} - 1\}$ . We apply the same procedure to  $Y_{2,I}$  with the sub-quantizer of step size  $q_2$ , and similarly  $v \in \{0, 1, ..., \sqrt{L} - 1\}$  is outputted. The output pair  $\{\omega, v\}$  is then mapped to one of L indices.

### B. Achievable rate and rate assignment with MLC

1) Computing achievable rates of CF: Achievable rates of CF versus the signal-to-noise ratio (SNR) of the source-to-destination link, SNR<sub>sd</sub>, is presented in Fig. 2 where both source and relay use  $2^m$ -QAM/PSK constellation with gray labeling. In [4], numerical results indicates that going beyond  $L=2^m$  does not yield any noticeable gains, so we make  $L=2^m$ .

When computing the achievable rate of CF with  $2^m$ -QAM,  $p(\hat{y}_2 = \{\omega, \upsilon\} | x_1)$ 

$$= \sum_{k=-\infty}^{\infty} \sum_{l=-\infty}^{\infty} \int_{(\omega+k\sqrt{L})q_1}^{(1+\omega+k\sqrt{L})q_1} \int_{(v+l\sqrt{L})q_2}^{(v+l\sqrt{L})q_2} p(y_2|x_1) dy_{2,I} dy_{2,R}$$

is involved. The maximum is obtained by numerical search over feasible input distributions  $p(x_1)$  and  $p(x_2)$ , as well as the quantization step size  $q_1$  and  $q_2$ . When both source and relay use  $2^m$ -PSK, even though the received signal is complex, we only need to quantize the phase of the received  $Y_2$ , and hence only one step size is involved in optimization. For comparison, we assume that  $\hat{Y}_2 = Y_2 + \hat{n}$  [9] instead of the nested scalar quantization, where  $\hat{n}$  is also Gaussian with zero mean and variance  $\hat{N}$ . The achievable rate for the case of  $\hat{Y}_2 = Y_2 + \hat{n}$  is maximized by a numerical search over feasible  $p(x_1)$ ,  $p(x_2)$  and  $\hat{N}$ . By observing Fig. 2, it is reasonable to conclude that it is sufficient to apply the nested scalar quantizer having  $L=2^m$  output indices at the relay.

2) Rate assignment: In the point-to-point channel, MLC [8] is implemented by splitting data stream into m bit-streams for  $2^m$ -ary constellation. Each sub-stream  $i \in \{1, 2, ..., m\}$  is encoded independently. At each time instance, the outputs of the (binary) encoders are combined to construct vector  $[A_1, A_2, ... A_m]$  which is then mapped to a constellation point X and transmitted. At the destination, Y is observed. The channel is described by conditional distribution p(y|x). The mutual information between the input and output is given by

$$I(X;Y) = I(A_1, A_2, ..., A_m; Y) = \sum_{i=1}^{m} I(A_i; Y | A^{i-1}), \quad (4)$$

where  $A^{i-1} \triangleq [A_1, A_2, ..., A_{i-1}]$  with  $A_0$  representing a constant, and a chain rule for the mutual information and a one-to-one relationship between X and  $[A_1, A_2, ..., A_m]$  are used. This equation suggests a multistage decoding, and the original channel is decomposed into m levels where the codeword of level i is decoded using the outputs of decoders of preceding levels. Therefore, the rate assigned to level i should be less than or equal to  $I(A_i; Y|A^{i-1})$ .

When MLC is implemented in the CF relay, which is presented in detail in section III, data stream at the source and quantized sequence at the relay both are split into m bit-streams. Each bit-stream at the source/relay is encoded/mapped to a binary codeword independently. If one-to-one relationships between  $X_1$  and  $[A_1, A_2, ..., A_m]$ ,  $\hat{Y}_2$  and  $[B_1, B_2, ..., B_m]$  and  $X_2$  and  $[C_1, C_2, ..., C_m]$  are assumed, multistage decoding will induce a decomposition of the original channel (3),

$$\sum_{i=1}^{m} R_i \le \max \sum_{i=1}^{m} I(A_i; B^m, Y_3 | C^m, A^{i-1}).$$
 (5)

Similarly, for level i, the assigned rate  $R_i$  should be less than or equal to  $I(A_i; B^m, Y_3 | C^m, A^{i-1})$ , and the constraint

$$I(Y_2; B_i | C^m, Y_3, B^{i-1}) \le I(C_i; Y_3 | C^{i-1})$$

should be satisfied. Under the same setup as the cases of Fig. 2, Fig. 3 and Fig. 4 show achievable rates of all levels which help to design code rates.

#### III. MULTILEVEL REALIZATION OF CF RELAY

In the following, the implementation of the CF relay using MLC will be described in detail.

## A. Encoding at the source

At the source, each data bit-stream is encoded with a length n binary LDPC code of rate  $R_i$  independently. At each time instance, binary vector  $[A_1,A_2,...A_m]$  is fed into a  $2^m$ -QAM/PSK modulator with power constraint  $P_s$ . The modulator maps  $[A_1,A_2,...A_m]$  to a symbol of the transmitted sequences  $\mathbf{X}_1$ .

## B. Quantization and encoding at the relay

At the relay, the received sequence  $\mathbf{Y}_2$  is quantized to a  $2^m$ -ary sequence  $\hat{\mathbf{Y}}_2$  of length n, where the symbol of  $\hat{\mathbf{Y}}_2$  has one-to-one relationship with binary vector  $[B_1, B_2, ... B_m]$ . Then  $\hat{\mathbf{Y}}_2$  is split into m bit-streams. The mapping is done by encoding each bit-stream through a systematic rate-1/2 LDPC code independently. The parity bits of the codeword approximate a random binning of the quantized sequence. The bit-streams corresponding to the random binning of different levels are combined via a  $2^m$ -QAM/PSK modulator similar to the one used at the source, to construct the sequence  $\mathbf{X}_2$ ; the symbol of  $\mathbf{X}_2$  has one-to-one relationship with binary vector  $[C_1, C_2, ... C_m]$ . The sequence  $\mathbf{X}_2$  will be transmitted to the destination at the next block.

# C. Decoding at the destination

A compound Tanner graphical model combining two (binary) LDPC Tanner graphs is proposed to perform joint iterative decoding of bits of each level. In the compound Tanner graphical model, information is exchanged not only within the component LDPC Tanner graphs individually, but also between the component LDPC Tanner graphs. In the following, the compound Tanner graphical model and information-exchange algorithm are depicted in detail.

1) Compound Tanner graphical model: When the sequence  $\mathbf{y}_3$  is observed, the destination searches for the codeword  $\mathbf{x}_1$  that maximizes the *a posteriori* probability  $p(\mathbf{x}_1|\mathbf{y}_3)$  by employing the bit-wise maximum *a posteriori* (MAP) decoder. The decoding rule for the bit-wise MAP decoder is

$$\hat{x}_{1,j} = \underset{x_{1,j} \in \mathcal{A}}{\operatorname{arg\,max}} \sum_{\sim x_{1,j}} p(\mathbf{x}_1 | \mathbf{y}_3),$$

for all j = 1, ..., n, where  $p(\mathbf{x}_1|\mathbf{y}_3)$  can be factorized as

$$p(\mathbf{x}_1|\mathbf{y}_3) = \frac{1}{p(\mathbf{y}_3)} \sum_{\hat{\mathbf{y}}_2, \mathbf{x}_2} p(\mathbf{x}_1, \mathbf{x}_2, \hat{\mathbf{y}}_2, \mathbf{y}_3), \tag{6}$$

$$\propto p(\mathbf{y}_3|\mathbf{x}_1,\mathbf{x}_2,\hat{\mathbf{y}}_2)p(\mathbf{x}_1,\mathbf{x}_2,\hat{\mathbf{y}}_2),$$
 (7)

$$\stackrel{(a)}{=} p(\mathbf{y}_3|\mathbf{x}_1,\mathbf{x}_2)p(\mathbf{x}_1,\mathbf{x}_2,\hat{\mathbf{y}}_2), \tag{8}$$

$$= p(\mathbf{y}_3|\mathbf{x}_1, \mathbf{x}_2)p(\mathbf{x}_2|\mathbf{x}_1, \hat{\mathbf{y}}_2)p(\hat{\mathbf{y}}_2|\mathbf{x}_1)p(\mathbf{x}_1), \tag{9}$$

$$\stackrel{(b)}{=} p(\mathbf{y}_3|\mathbf{x}_1,\mathbf{x}_2)p(\mathbf{x}_2|\hat{\mathbf{y}}_2)p(\hat{\mathbf{y}}_2|\mathbf{x}_1)p(\mathbf{x}_1), \tag{10}$$

$$\overset{(c)}{\propto} p(\mathbf{y}_3|\mathbf{x}_1, \mathbf{x}_2) p(\hat{\mathbf{y}}_2|\mathbf{x}_1) \mathbb{1}\{\mathbf{x}_2 \cup \hat{\mathbf{y}}_2 \in \mathcal{C}_{\mathbf{R}}\} \mathbb{1}\{\mathbf{x}_1 \in \mathcal{C}_{\mathbf{S}}\}, \tag{11}$$

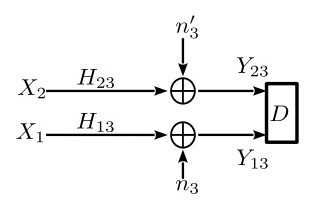


Fig. 5. The simplified destination part of the channel model

where (a) follows that  $\mathbf{y}_3$  is only dependent on  $\mathbf{x}_1$  and  $\mathbf{x}_2$ . (b) follows that  $\mathbf{x}_1 \leftrightarrow \hat{\mathbf{y}}_2 \leftrightarrow \mathbf{x}_2$  forms a Markov chain. (c) is due to the fact that  $\mathbf{x}_1$  must be a codeword in code book  $\mathcal{C}_{\mathbf{S}}$ , and  $(\mathbf{x}_2 \cup \hat{\mathbf{y}}_2)$  must be a codeword in code book  $\mathcal{C}_{\mathbf{R}}$ .

and  $(\mathbf{x}_2 \cup \hat{\mathbf{y}}_2)$  must be a codeword in code book  $\mathcal{C}_{\mathbf{R}}$ . At block t, the destination receives polluted  $X_2^{(t-1)}$  containing side information about  $X_1^{(t-1)}$  which is independent of  $X_1^{(t)}$ . Due to this independence, by applying successive interference cancellation, the destination part of the channel model can be simplified as [6],

$$Y_{23}^{(t)} = H_{23}X_2^{(t-1)} + n_3', (12)$$

$$Y_{13}^{(t)} = H_{13}X_1^{(t)} + n_3, (13)$$

which is shown in Fig. 5. At block t, the destination first jointly decodes  $\mathbf{X}_1^{(t-1)}$  and  $\mathbf{X}_2^{(t-1)}$  on the basis of  $\mathbf{Y}_{23}^{(t)}$  and  $\mathbf{Y}_{13}^{(t-1)}$  where  $\mathbf{Y}_{23}^{(t)}$  is got by treating  $\mathbf{X}_1^{(t)}$  as Gaussian noise of zero mean and power  $H_{12}^2 P_s$ , and  $\mathbf{Y}_{13}^{(t-1)}$  comes by subtracting  $\mathbf{X}_2^{(t-2)}$  decoded at block t-1 from  $\mathbf{Y}_3^{(t-1)}$ . This operation can separate  $Y_3^{(t)}$  to two orthogonal links  $Y_{13}^{(t)}$  and  $Y_{23}^{(t)}$  with independent AWGN  $n_3'$  of variance  $N_3 + H_{12}^2 P_s$  and  $n_3$  of variance  $N_3$ . Therefore, (11) can be decoupled as

$$p(\mathbf{y}_{13}|\mathbf{x}_1)p(\mathbf{y}_{23}|\mathbf{x}_2)p(\mathbf{\hat{y}}_2|\mathbf{x}_1)\mathbb{1}\{\mathbf{x}_2\cup\mathbf{\hat{y}}_2\in\mathcal{C}_{\mathbf{R}}\}\mathbb{1}\{\mathbf{x}_1\in\mathcal{C}_{\mathbf{S}}\},$$

(14)

$$\stackrel{(d)}{=} \prod_{j=1}^{n} p(y_{13,j}|x_{1,j}) \prod_{k=1}^{n} p(y_{23,k}|x_{2,k}) \prod_{l=1}^{n} p(\hat{y}_{2,l}|x_{1,l}) \cdot \mathbb{1}\{\mathbf{x}_{2} \cup \hat{\mathbf{y}}_{2} \in \mathcal{C}_{\mathbf{R}}\} \mathbb{1}\{\mathbf{x}_{1} \in \mathcal{C}_{\mathbf{S}}\}, \quad (15)$$

where (d) is due to the fact that relay channel is i.i.d. and scalar quantizer is employed by the relay. From the decomposition, it is observed that the joint decoding is implemented by connecting two decoding procedures based on  $p(y_{13}|x_1)$  and  $p(y_{23}|x_2)$  respectively with the function  $p(\hat{y}_2|x_1)$ .

Based on the conditional distributions  $p(y_{13}|a^{i-1},a_i)$ ,  $p(y_{23}|c^{i-1},c_i)$ , and  $p(b_i|a_i)$ , level i performs the (binary) joint decoding by conducting an information-exchange algorithm in the compound Tanner graphical model composed of two LDPC Tanner graphs. The model is shown in Fig. 6. The Graph S is for the source. The Graph S is for the relay. The variable nodes of two LDPC Tanner graphs are connected by function nodes  $Q_i$ . These nodes  $Q_i$  represent  $p(b_i|a_i)$  which is corresponding to the information exchanged between two LDPC Tanner graphs.

2) Information-exchange algorithm: The message passing rules within LDPC Tanner graph remains the same. By setting

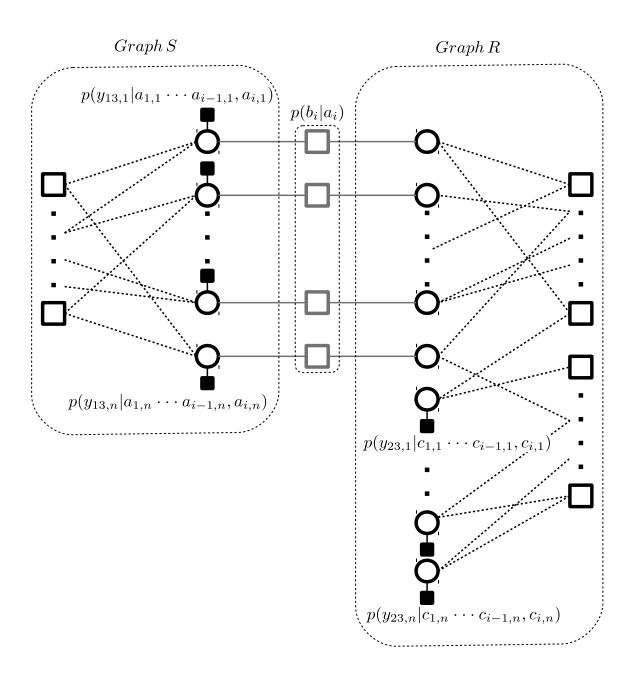


Fig. 6. The compound Tanner graph for decoding bits of level i

messages exchanged among nodes to be in *log likelihood ratio* (LLR) form, the sum-product algorithm can be conducted. The message passing rules between variable nodes of *Graph S* and *Graph R* through the function nodes  $Q_i$  is derived as follows. The LLRs passed from  $Q_i$  to  $a_i$  and  $b_i$  are given by

$$LLR_{Q_{i}\to a_{i}} = ln \frac{p(0|0) \cdot p(b_{i}=0) + p(1|0) \cdot p(b_{i}=1)}{p(0|1) \cdot p(b_{i}=0) + p(1|1) \cdot p(b_{i}=1)},$$

$$= ln \frac{p(0|0) \cdot e^{LLR_{b_{i}\to Q_{i}}} + p(1|0)}{p(0|1) \cdot e^{LLR_{b_{i}\to Q_{i}}} + p(1|1)},$$

$$LLR_{Q_{i}\to b_{i}} = ln \frac{p(0|0) \cdot p(a_{i}=0) + p(0|1) \cdot p(a_{i}=1)}{p(1|0) \cdot p(a_{i}=0) + p(1|1) \cdot p(a_{i}=1)},$$

$$= ln \frac{p(0|0) \cdot e^{LLR_{a_{i}\to Q_{i}}} + p(0|1)}{p(1|0) \cdot e^{LLR_{a_{i}\to Q_{i}}} + p(1|1)},$$
(17)

where  $e^{LLR_{a_i \to Q_i}}$  and  $e^{LLR_{b_i \to Q_i}}$  denotes the LLRs passed from variable nodes  $a_i$  and  $b_i$  to function node  $Q_i$ .

Based on the above mentioned message-passing rules, the destination first initializes  $p(y_{13}|a^{i-1},a_i)$  and  $p(y_{23}|c^{i-1},c_i)$ according to channel observations and previous decoded bits  $a^{i-1}$  and  $c^{i-1}$ . With initialized LLRs, by running traditional sum-product algorithm for  $I_S$  local iterations, the Graph S updates  $e^{LLR_{a_i \to Q_i}}$  which is passed to the Graph R based on the message-passing rule depicted in (17). Once receiving  $LLR_{Q_i \to b_i}$  together with initialized LLRs, the Graph R runs traditional sum-product algorithm for  $I_R$  local iterations to get the updated  $e^{LLR_{b_i \to Q_i}}$  which is passed to the *Graph S* to help the following  $I_S$  local iterations through the messagepassing rule depicted in (16). With appropriate  $I_S$  and  $I_R$  local iterations as well as  $I_G$  global iterations, the decoder outputs decoded bits  $a_i$  and  $b_i$  by making hard decisions on LLRs  $e^{LLR_{a_i\to Q_i}}$  and  $e^{LLR_{b_i\to Q_i}}$ . And these decoded bits are used in decoding of following levels.

#### IV. SIMULATION RESULTS

In this section, the simulation results for the CF relay with 16-QAM or 16-PSK constellation are presented. Parameters are set to  $N_3=1,\ N_2=8,\ H_{13}=1,\ H_{12}=2,$  and  $H_{23}=1$ . The power of the source and relay is assumed to be the same throughout the experiments. The SNRs of the system are changed by keeping all the other parameters constant and varying the power of the source (equivalently, the relay).

DVB-S2 LDPC codes of blocklength 64800 are used as component codes at the source. At the relay, two rate-1/2 DVB-S2 LDPC codes are concatenated for mapping each quantized bit-stream. One of the rate-1/2 DVB-S2 LDPC codes is used to encode the first 32400 quantized bits, and the other one is used to encode the rest quantized bits. Then the parity bits are concatenated for transmission.

In order to provide transparency and repeatability of experiments, we opted to use standard code components. This naturally circumscribes the set of available rates for experiments. For our experiment, the transmission of 3.4 bits/s is chosen for 16-QAM, and 3.27 bits/s is chosen for 16-PSK. The corresponding SNR<sub>sd</sub> are approximately 9.68dB for 16-QAM and 11.6dB for 16-PSK (see Fig. 2), whose optimal rates assigned to each level from the most significant bit to least significant bit are [0.9, 0.8, 0.9, 0.8] for 16-QAM and [0.9, 0.9, 0.8, 2/3] for 16-PSK (see Fig. 3 and Fig. 4).

For comparison, BICM applied in [6] and [7] is also simulated, where component LDPC codes of the same rate are used in all sub-channels. The transmission of 3.33 bits/s is chosen for 16-QAM, and the DVB-S2 LDPC code of rate 5/6 is used. The transmission of 3.2 bits/s is chosen for 16-PSK, and the DVB-S2 LDPC code of rate 0.8 is used.

Fig. 7 shows the bit-error-rate (BER) performances of the CF relay using MLC and BICM. The horizontal axis shows the source-destination SNR, which is related to the other link SNRs through the relationship mentioned at the beginning of this section. It is observed that for both 16-QAM and 16-PSK MLC has a better performance than BICM, even though we simulate the CF relay using BICM at lower rates. This is because the same LDPC code can not provide enough error protection for the weak sub-channel of BICM, while the LDPC code of optimal rate is selected for the corresponding level of MLC.

In the CF relay using MLC, the waterfall for the BER of 16-QAM and 16-PSK occurs at approximately 10.62dB and 13.75dB respectively. The gap between theory and experiment is 0.94dB for 16-QAM and 2.15dB for 16-PSK. The gap is due to two factors: one of them is the shaping gain, because our technique (for practicality purposes) does not use vector quantization. It is noteworthy that this loss occurs only for relay transmission (which is subject to quantization), therefore the shaping loss is smaller than 1.5dB. Second, the DVB-S2 LDPC code does not perform exactly at the Shannon limit.

#### V. CONCLUSION

We have proposed a full-duplex CF relay scheme using MLC. The quantized sequence is obtained through the nested

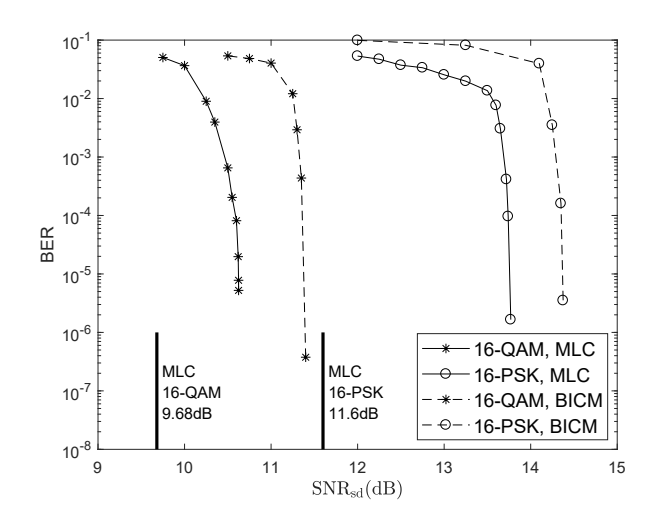


Fig. 7. 16-QAM and 16-PSK simulation results with  $N_3=1,\ N_2=8,\ H_{13}=1,\ H_{12}=2,\ H_{23}=11,$  and  $P_r=P_s.$ 

scalar quantization, and then directly mapped to a transmission sequence at the relay. A compound Tanner graphical model and corresponding information-exchange algorithm are derived for joint decoding at the destination. For implementation, DVB-S2 LDPC codes of different rates are selected by the source according to the optimal rates of different levels, and the rate-1/2 DVB-S2 LDPC code is used to map the quantized sequence. The simulation results show using MLC has a better performance than using BICM, and the use of scalar quantization and DVB-S2 LDPC code leads to the gap between theory and experiment.

## REFERENCES

- E. van der Meulen, "Three-terminal communication channels," Adv. Appl. Probab., vol. 3, pp. 120–150, 1971.
- [2] T. Cover and A. E. Gamal, "Capacity theorems for the relay channel," IEEE Trans. Inf. Theory, vol. 25, no. 5, pp. 572–584, Sep. 1979.
- [3] M. Uppal, Z. Liu, V. Stankovic, and Z. Xiong, "Compress-forward coding with BPSK modulation for the half-duplex Gaussian relay channel," *IEEE Trans. Signal Process.*, vol. 57, no. 11, pp. 4467–4481, Nov. 2009.
- [4] J. Amjad, M. Uppal, and S. Qaisar, "Multi-level compress and forward coding for half-duplex relays," in *Proc. IEEE Globecom*, Anaheim, CA, USA, Dec. 2012, pp. 4536–4541.
- [5] R. Blasco-Serrano, R. Thobaben, M. Andersson, V. Rathi, and M. Skoglund, "Polar codes for cooperative relaying," *IEEE Trans. Commun.*, vol. 61, no. 2, pp. 3263–3273, Feb. 2015.
- [6] V. Nagpal, I.-H. Wang, M. Jorgovanovic, D. Tse, and B. Nikolić, "Quantize-map-and-forward relaying: Coding and system design," in Proc. 48th Annual Allerton Conference on Communication, Control, and Computing, Allerton, IL, USA, Oct. 2010, pp. 443–450.
- [7] V. Nagpal, I.-H. Wang, and M. Jorgovanovic, "Coding and system design for quantize-map-and-forward relaying," *IEEE J. Sel. Areas Commun.*, vol. 31, no. 8, pp. 1423–1435, Aug. 2013.
- [8] H. Imai and S. Hirakawa, "A new multilevel coding method using error correcting codes,," *IEEE Trans. Inf. Theory*, vol. 23, no. 3, pp. 371–377, May 1977.
- [9] A. El Gamal and Y.-H. Kim, Network Information Theory, 1st ed. Cambridge, U.K: Cambridge University Press, 2012.
- [10] Z. Liu, S. Cheng, A. Liveris, and Z. Xiong, "Slepian-wolf coded nested lattice quantization for Wyner-Ziv coding: High-rate performance analysis and code design," *IEEE Trans. Inf. Theory*, vol. 52, no. 10, pp. 4358–4379, Oct. 2006.